EXPLORATORY NUMERICL STUDY OF LIQUID HYDROGEN HAZARDS

Baopeng Xu and Jennifer X. Wen

Fire and Explosion Modelling Group (FMEG)

School of Mechanical Engineering Sciences, University of Surrey, Guildford, UK

ABSTRACT

Hydrogen is one of a handful of new, low carbon solutions that will be critical for the transition to net zero. The upscaling of production and applications entails that hydrogen is likely to be stored in liquid phase (LH_2) at cryogenic conditions to increase its energy density. Widespread LH_2 use as an alternative fuel will require significant infrastructure upgrades to accommodate increased bulk transport, storage, and delivery. However, current LH_2 bulk storage separation distances are based on subjective expert recommendations rather than experimental observations or physical models. Experimental studies of large-scale LH_2 release are challenging and costly. The existing large-scale tests are scarce and numerical studies are a viable option to investigate the existing knowledge gaps.

Controlled or accidental releases of LH_2 for hydrogen refueling infrastructure would result in high momentum two-phase jets or formation of liquid pools depending on release conditions. Both release scenarios lead to a flammable/explosive cloud, posing a safety issue to the public.

The manuscript reports exploratory study to numerically determine the safety zone resulting from cryogenic hydrogen releases related to LH_2 storage and refueling using the in-house HyFOAM solver further modified for gaseous hydrogen releases at cryogenic conditions and the subsequent atmospheric dispersion and ignition within the platform of OpenFOAM V8.0. The current version of the solver neglects the flashing process by assuming that the temperature of the stored LH_2 is equal to the boiling point at the atmospheric condition. Numerical simulations of dispersion and subsequent ignition of LH_2 release scenarios with respect to different release orientations, release rates, release temperatures and weather conditions were performed. Both hydrogen concentration and temperature fields were predicted, and the boundary of zones within the flammability limit was also defined. The study also considered the sensitivities of the consequences to the release orientation, wind speed, ambient temperature, and release content, etc. The effect of different barrier walls on the deflagration were also evaluated by changing the height and location.

Keywords: Liquid hydrogen; HyFOAM; jet; jet flames; vapour cloud explosions.

1. INTRODUCTION

Hydrogen, as a clean energy carrier, is frequently stored in liquid phase (LH_2) at cryogenic conditions to increase its energy density. Controlled or accidental releases of LH_2 for hydrogen refueling infrastructure at airports would result in high momentum two-phase jets or formation of liquid pools depending on release conditions. Both release scenarios lead to a flammable/explosive cloud, posing a safety issue to the public.

Widespread LH_2 use as an alternative fuel will require significant infrastructure upgrades to accommodate increased bulk transport, storage, and delivery. However, current LH_2 bulk storage separation distances are based on subjective expert recommendations rather than experimental observations or physical models. Experimental studies of large-scale LH_2 release are tedious, expensive, and dangerous tasks. The existing large-scale tests are scarce and numerical studies are a viable option to investigate the existing knowledge gaps.

LH_2 is typically −252.87 °C and below the freezing temperature of oxygen (O_2) (-218.8 °C). It evaporates with a volume expansion of 1:848. As hydrogen is flammable over a wide range (4-76% by volume), the risk of ignition and associated fire and explosion need to be carefully addressed. LH_2 is typically stored in pressures from 10 to around 35 bar, ignition of accidentally released LH_2 would result in jet fires. Delayed ignition is likely to result in hydrogen explosions. Catastrophic failure of the storage tanks could result in massive LH_2 releases, forming large flammable could, which might lead to serious cascading events with serious consequences for the airport.

Limited research concerning LH_2 safety has been conducted by NASA in the 1980s [1] focusing on spills, and in recent years by projects funded through US Department of Energy on LH_2 jets and jet fires, the HSE Science Division on both ignited and unignited releases of LH_2. The state of the art has been considerably enhanced by recently completed pan European project "Pre-normative research for safe use of liquid hydrogen (PRESLHY)" [2] funded by FCH 2 JU. Relevant to the proposed research, more than 100 ignited and unignited cryogenic gaseous hydrogen jets have been tested. The measurements have been used to assist development and validation of CFD based models and engineering correlations. Twenty-three large scale tests were also conducted whereby LH_2 was released into a steel frame with two levels of congestions [3]. The results also demonstrated that an increasing hydrogen inventory, either through an increased release pressure or larger nozzle, can result in a more serious event upon ignition.

Published CFD models with validation for cryogenic hydrogen gas mainly involve unignited [2,5] and ignited jets [6,7]. Few CFD simulations involving LH_2 are available in the open literature covering only pool spread [8,9].

The above analysis highlights the urgent need to address the following challenges related to LH_2 storage and transferring facilities, which will be addressed in the present exploratory numerical study:

- Horizontal and vertical extents of the flammable cloud following accidental LH_2 release.
- Fire and explosion hazards associated with the above.
- Explosion hazards associated with catastrophic failure of LH_2 storage tanks.

2. AN OVERIEW OF MODELING OF ATMOSPHERIC DISPERSION AND IGNITION OF LARGE-SCALE LH_2 RELEASES

Jet releases and instantaneous releases are two typical release scenarios. A jet release occurs when a small rupture or a venting pipe exists in the storage system, while an instantaneous release corresponds to an abrupt failure of a storage tank. LH_2 is stored several bars above atmospheric pressure. Therefore, A LH_2 release is accompanied by a spontaneous flash evaporation, resulting in a two-phase mixture. An instantaneous release of large amount of LH_2 would lead to the formation of a LH_2 pool. The LH_2 pool is heated via the heat transfer from the solid ground/walls, ambient air and the sun radiation. In the

initial stage of the evaporation process, the conduction heat transfer via the ground is the major contribution due to the very large temperature difference, which results in fast vaporization due to the violent boiling. The evaporated gaseous hydrogen is dispersed in the ambient air, forming a dense cloud. The atmospheric dispersion leads to a formation of a flammable/explosive cloud, which is a safety issue to the public. The accurate prediction of the atmospheric hydrogen distribution is an important task of accurate hazard assessments of storage systems.

Numerical predictions of the atmospheric dispersion of the instantaneous release require the determination of the pool size and its evaporation rate. The catastrophic failure of a storage tank is the most dangerous release scenarios, which causes an instantaneous release of LH_2. To retard the spread of LH_2 and to limit the vaporization rate, a detention pit is intended to be used to minimize the size of the flammable vapor cloud which must be dispersed to nonflammable concentrations. In this study, the atmospheric dispersion of vaporized LH_2 is numerically studied for the instantaneous release scenarios and with/without detention pits. Following validation using data from NASA LH_2 tests, the numerical predictions were used to analyze the effects of ambient temperature, atmospheric conditions and presence of a retention pit on flammable cloud dispersion and associated potential hazardous distances.

During a jet release of LH_2, abrupt flash evaporation of occurs at the release point due to its superheat and subsequently it quickly transitions to a single-phase jet mainly due to the mixing with air. At proximity of the release point the temperature is below the air liquefaction temperature (77 K) or even the solidification temperature of air (58 K). Phase transitions of oxygen and nitrogen might occur. The jet momentum decays due to the mixing with ambient air, and then the momentum-dominant jet gradually transitions to a buoyancy-dominant jet. The weather conditions play important role to the dispersion process by both diluting the dispersed cloud and altering the buoyant effect. Moreover, if air humidity is considered, the condensation of water vapor increases the buoyant effect due to the released latent heat.

In this study the phase transitions are neglected, and focus is on the atmospheric dispersion of jet releases under different weather conditions. An in-house CFD code is used here, specifically written for simulating atmospheric dispersion of cryogenic jet releases, incorporating the buoyancy effect and atmospheric boundary condition. The code was previously validated [8] against NASA test data [1]. The released jet flow induces high turbulence that significantly enhanced the mixing. The fast mixing elevates the temperature of the hydrogen cloud. Therefore, an assumption of ideal gas was made for the solved mixture. In addition, a gaseous inlet boundary is used by ignoring the air mixing prior to the inlet boundary and conserving the release momentum.

2. METHODOLOGY

The development built on from the previous simulations of the authors' group for hydrogen flash fire [10] and hydrogen gas explosion in the presence of obstacles [11]. Numerical modeling of LH_2 releases, subsequent atmospheric dispersion and ignition is challenging, particularly for the phase change dynamics. The mixing of cryogenic hydrogen with ambient air can result in phase transitions of oxygen and nitrogen at the near-field, which is too complicated to be directly modeled due to the cryogenic condition and lack of validations and accuracy. The phase transition of oxygen and nitrogen occurs only at the near-field, so its effect to the far-field dispersion should be limited. Furthermore, the condensation of water vapor prevails in the dispersion process, which releases its latent heat to increase the cloud buoyancy. It was also experimentally revealed the warming from the mixing with air plays a major role in the buoyancy effect. Therefore, in this work, the humidity is neglected.

Three-dimensional multi-component compressible Reynolds-averaged Navier-Stokes equations were formulated:

$$\frac{\partial \bar{\rho}}{\partial t} + \nabla \cdot (\bar{\rho}\overline{\boldsymbol{u}}) = 0 \tag{1}$$

$$\frac{\partial \bar{\rho}\overline{u}}{\partial t} + \nabla \cdot (\bar{\rho}\overline{\boldsymbol{u}}\overline{\boldsymbol{u}}) = -\Delta \bar{p} + \nabla \cdot \overline{\tau_{eff}} + \bar{\rho}\boldsymbol{g} \tag{2}$$

$$\frac{\partial \bar{\rho}\overline{Y_l}}{\partial t} + \nabla \cdot (\bar{\rho}\bar{\boldsymbol{u}}\overline{Y_l}) = \nabla \cdot \left(\mu_{eff}\overline{Y_l}\right) + \dot{Y}_l^C \quad (3)$$

$$\frac{\partial \bar{\rho}\overline{h_s}}{\partial t} + \nabla \cdot \left(\bar{\rho}\bar{\boldsymbol{u}}\overline{h_s}\right) = \nabla \cdot \left(\alpha_{eff}\nabla\overline{h_s}\right) + \sum_{i=1}^{n}\left(\nabla \cdot \overline{h_{sl}}[\rho D_i - \alpha]\nabla\overline{Y_l}\right) + \dot{Q}^C \quad (4)$$

$$\frac{\partial (\bar{\rho}k)}{\partial t} + \nabla \cdot (\bar{\rho}\bar{\boldsymbol{u}}k) = \nabla \cdot \left[\left(\frac{\mu_{eff}}{Pr_k}\right)\nabla k\right] + P_k + G_k - \bar{\rho}\varepsilon \quad (5)$$

$$\frac{\partial (\bar{\rho}\varepsilon)}{\partial t} + \nabla \cdot (\bar{\rho}\bar{\boldsymbol{u}}\varepsilon) = \nabla \cdot \left[\left(\frac{\mu_{eff}}{Pr_\varepsilon}\right)\nabla\varepsilon\right] + \frac{\varepsilon}{k}(C_{\varepsilon 1}P_k + C_{\varepsilon 1}C_{\varepsilon 3}G_k - C_{\varepsilon 2}\varepsilon) \quad (6)$$

Where $\rho, \boldsymbol{u}, p, Y_l, h_s, g, k, \varepsilon$ are respectively density, velocity vector, pressure, species mass fraction, sensible enthalpy, gravity, turbulent energy and its dissipation rate, $\dot{Y}_l^C$ *and* $\dot{Q}^C$ are chemical source terms. In the above formulations the turbulent effect is modeled by standard time-averaged $k-\varepsilon$ model. The chemical source terms are closed by the EDC combustion model along with a detailed kinetic scheme involving 9 species and 19 steps. The radiative heat transfer is not considered in the current study.

3. RESULTS

LH_2 jet releases of constant rate were considered involving both horizontal and vertical jet releases of different wind speeds. A summary of the considered cases is provided in Table 1.

Table 1. The simulated cases

Case ID	Description	Nozzle/pool size	Release rate/content	Temperature (K)	Wind (m/s)
HJR1	Horizontal jet release	96 × 96 mm^2	2900 kg/h	25	0
HJR2					3
HJR3					13
VJR1	Vertical jet release	41 × 41 mm^2	520 kg/h	25	0
VJR2					13

To simplify mesh generations, round hydrogen inlets were replaced with squared inlets of the same area. It was found in a preliminary simulation that the simulated jet quickly evolved into a round jet for a squared inlet. This simplification can significantly reduce the computational cost and increase the code convergence without losing accuracy as well. To reduce the computational cost, only half of the domains were simulated with a symmetric boundary condition. Grid refinement was made along the release direction.

Two kinds of inlet boundary conditions were respectively adopted for the wind inlet and the hydrogen inlet. A neutral atmospheric boundary condition [8], was applied on the left plane of the computational domain, and a velocity inlet boundary condition with 2% turbulent intensity was set for the hydrogen inlet boundary. For the horizontal releases the right and front planes were set as an inlet-outlet boundary condition, and a slip boundary condition was used for the top plane. While for the vertical releases an inlet-outlet boundary condition was applied at the right, front and top planes. A no-slip, adiabatic boundary condition was applied on the ground for all the cases.

The effect of air humidity on the dispersion were not considered in this work. Ambient air was assumed to have a temperature of 293 K and zero humidity. A still flow field was initially set for all the case. For the cases of wind speeds, hydrogen was injected only after a stable wind field was attained across the computational domain. Finally, transient simulations were performed until stable results were achieved for all the cases.

The fields of temperature and hydrogen concentration were computed, and the dispersed clouds within

the lower flammability limit (LFL, 4% by volume) and lower explosive limit (LEL, 10% by volume) were also defined. All the units of X and Z axis in the follow figures are in metres.

3.1 Unignited horizontal jet releases

This scenario is a horizontal release with a release velocity of 90 m/s. The release point is located 1 m away from the left boundary and 5 m above the ground. Figure 1 shows the predicted contour of temperature for different wind speeds. The white line is an isoline of the low flammability limit. The jet release is initially momentum-dominant and gradually loses its momentum due to the mixing with ambient air and then shows a buoyant effect. The buoyancy effect is significantly restrained by a concurrent wind condition (both HJR2 and HJR2). The predicted jet of HJR2 is slightly lifted upwards and extends further downstream. The buoyancy effect completely diminishes for the case of HJR3. A strong wind condition also greatly enhances the mixing, reducing the size of the dispersed cloud for the case of HJR3. The released jets have a low-temperature core below 200 K extending to 10 m beyond the release point.

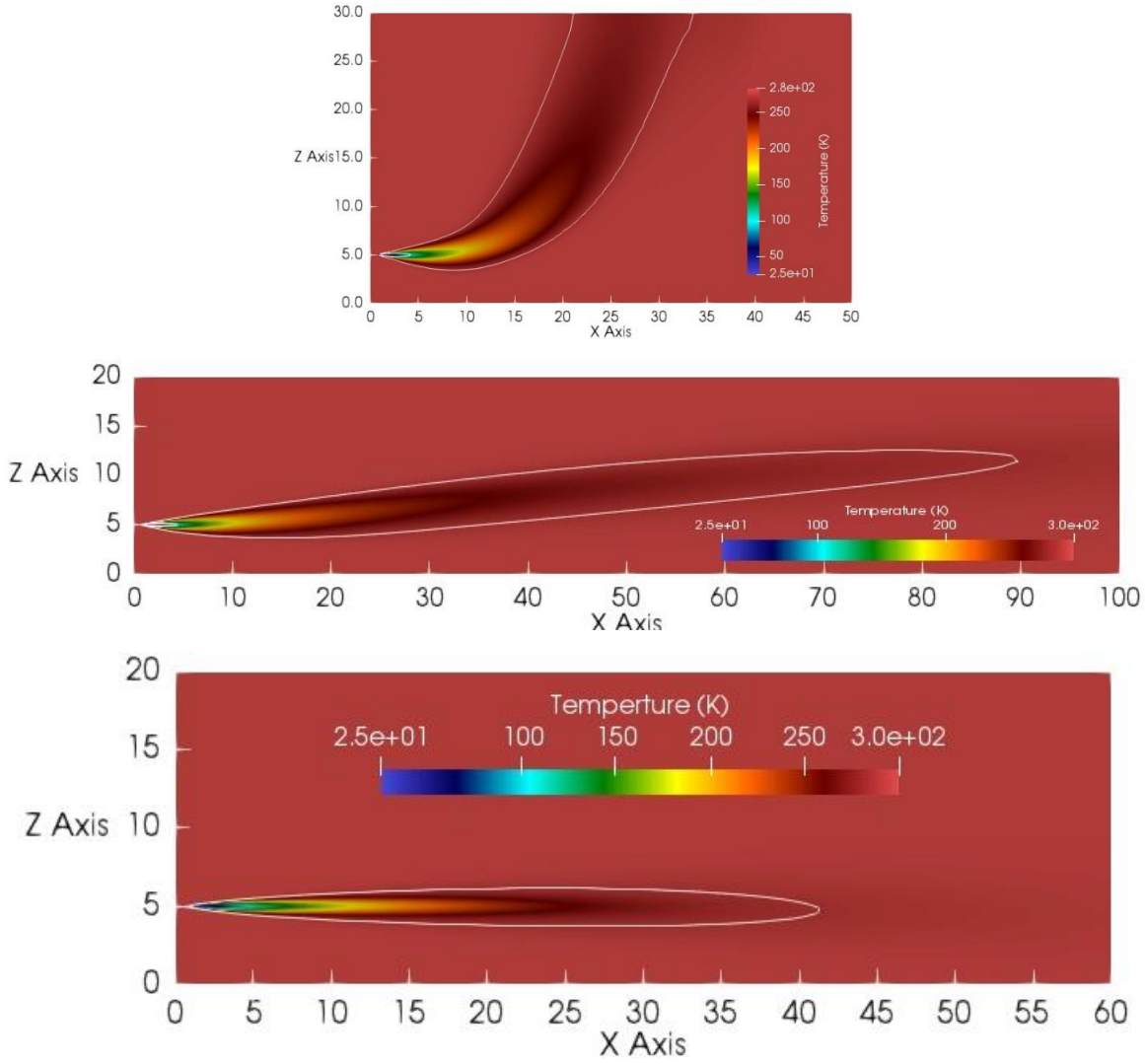

Figure 1. Predicted contour of temperature overlapped with the flammability limits for the cases of HJR1 (top), HJR2 (middle) and HJR3 (bottom).

3.2 Unignited vertical jet releases

This scenario is an upward release with a release velocity of 90 m/s. Figure 2 shows the predicted contour of temperature for the cases of VJR1 and VJR2. For the case of VJR1 with no wind condition the release momentum is in alignment with the buoyancy force, the jet flow slowly decays upwards. For the case of VJR2 with the strong wind condition, the strong cross wind greatly enhances the mixing, resulting in a quick decay of the release momentum. The predicted cloud turns to be horizontal and quickly disperses into the ambient air.

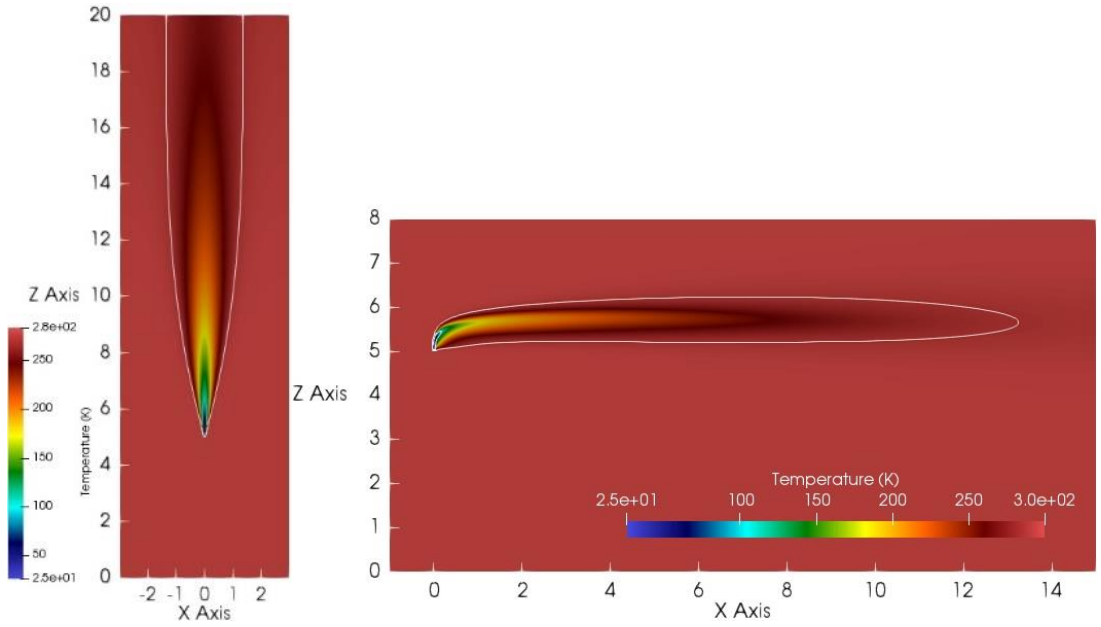

Figure 2. Predicted contour of temperature overlapped with the flammability limits for the cases of VJR1 (left) and VJR2 (right).

3.3 Ignited horizontal jet releases – jet fires

Two horizontal jet releases, i.e. HJR1 and HJR2, were immediately ignited after the releases. The predicted contours of temperature and H2 mass fraction in the middle plane for the cases of HJR1 and HJR2 are shown in Figures 3 and 4, respectively. A jet fire establishes for both cases. The horizontal extend of the jet fires is much smaller than that of the corresponding unignited cases. The chemical reaction not only consumes hydrogen, but also significantly increases the buoyant effect. The momentum-driven jet fire quickly transitions to be buoyancy-dominant for the case of HJR1. Under a wind condition the buoyant effect is significantly reduced and a tilted long jet fire is predicted.

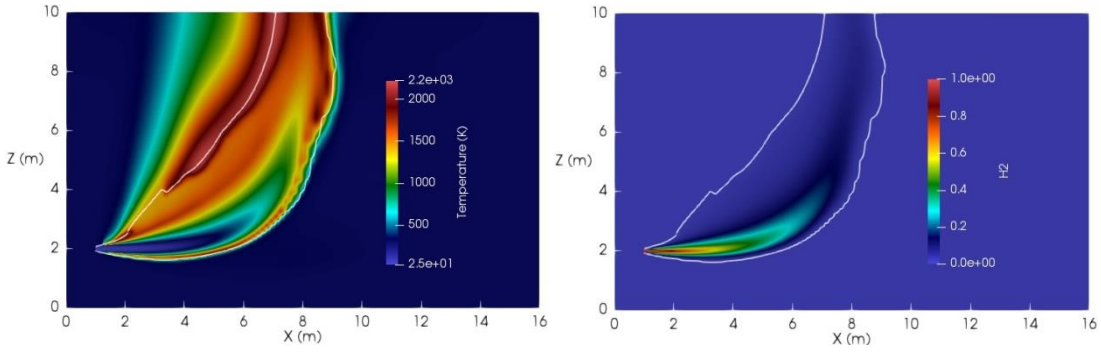

Figure 3. Predicted contours of temperature and H2 mass fraction in the middle plane for the case of HJR1. (White lines stand for the lower flammability limit)

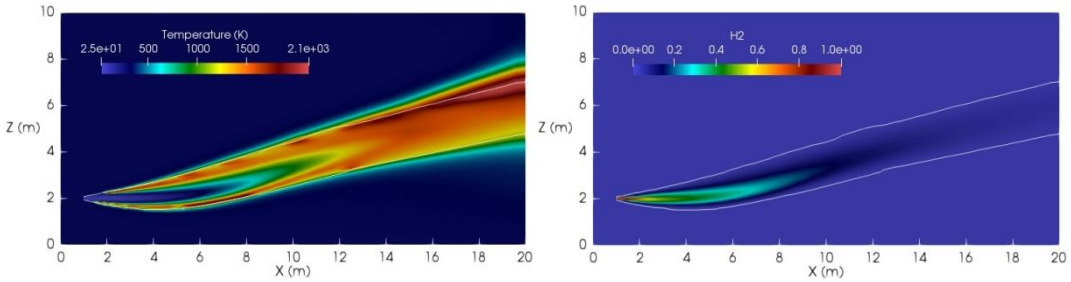

Figure 4. Predicted contours of temperature and H2 mass fraction in the middle plane for the case of HJR2. (White lines stand for the lower flammability limit).

3.4 Ignited vertical jet release – jet fire

The vertical jet release of VJR1 was immediately ignited after the releases. The predicted contours of temperature, H2 mass fraction and velocity in the middle plane for the cases of VJR1 are shown in Figure 5, respectively. A vertical jet fire was predicted. The predicted flame height is 15 meters, which is higher than a normal hydrogen jet fire due to its cryogenic temperature.

It is worth mentioning that the predicted over-pressures for both the horizontal and vertical jet fires are small. A simulation with a delayed ignition was conducted for the horizontal release of HJR1 and no significant over-pressure was predicted.

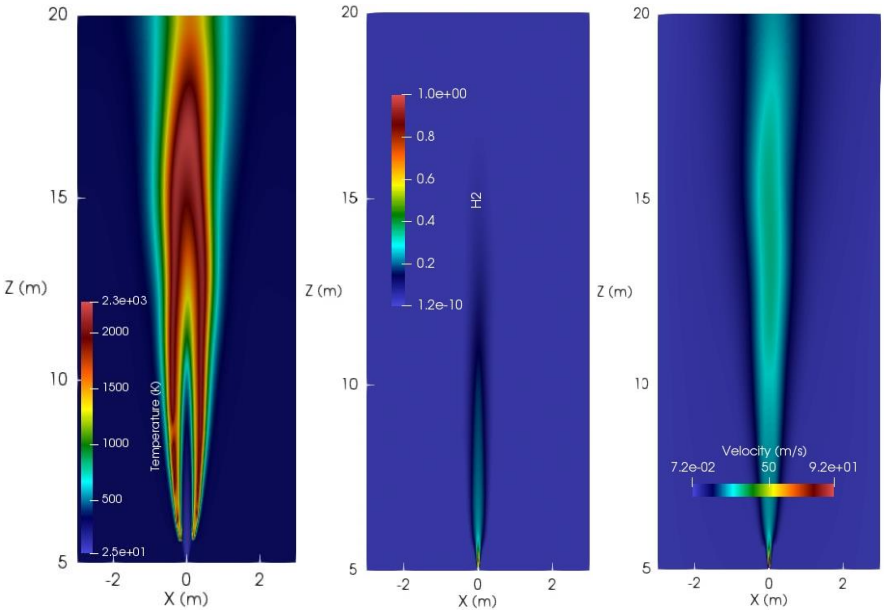

Figure 5. Predicted contours of temperature, H2 mass fraction and velocity in the middle plane for the case of VJR1.

3.5 Vapour cloud explosions following instantaneous releases

The hydrogen vapour cloud resulting from the instantaneous releases of 600 kg which resulted in 8 × 8 m^2 square pool in no wind condition (IR9) and under wind speed of 3 m/s (IR10) were firstly simulated using the same model developed by the authors and reported in [8]. The predicted clouds were used to investigate the explosive hazards associated with ignited instantaneous releases. The effects of blast walls as well as their heights and locations on mitigating the effects of potential explosions were also evaluated for the case of IR10 with wind speed of 3 m/s by setting up a barrier wall of two heights (5

m and 10 m) and two locations (30 m and 40 m). The coordinate origin is located at the pool center. The ignition source is a sphere of a radius of 0.5 m located at (25, 0, 5) for all the cases. Ignition is activated at 40 s after the release by gradually increasing the temperature of the ignition cells to 1800 K within 0.01 s. The total ignition time was set to be 0.5 s.

Figure 6 shows the predicted contours of temperature for the case of IR10 at t = 40 s prior to the ignition. The wind speed for this case is 3 m/s. The predicted clouds are lifted off and the cloud is deflected by the barrier wall.

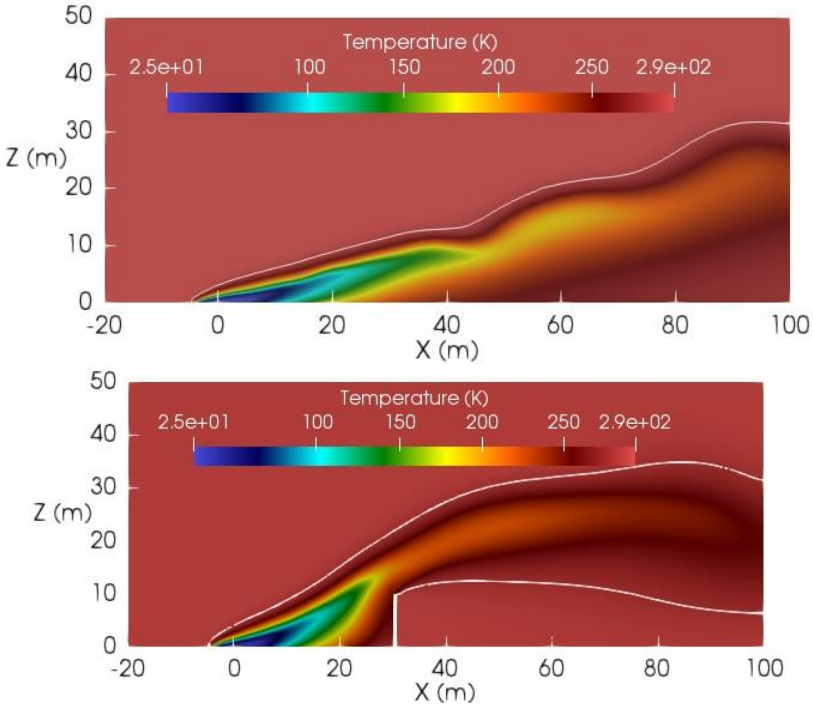

Figure 6. Predicted contour of temperature overlapped with the lower flammability limit for the case of IR10 at t = 40 s prior to the ignition. (The top for the case with no barrier wall and the bottom for the case with a 10 m barrier wall)

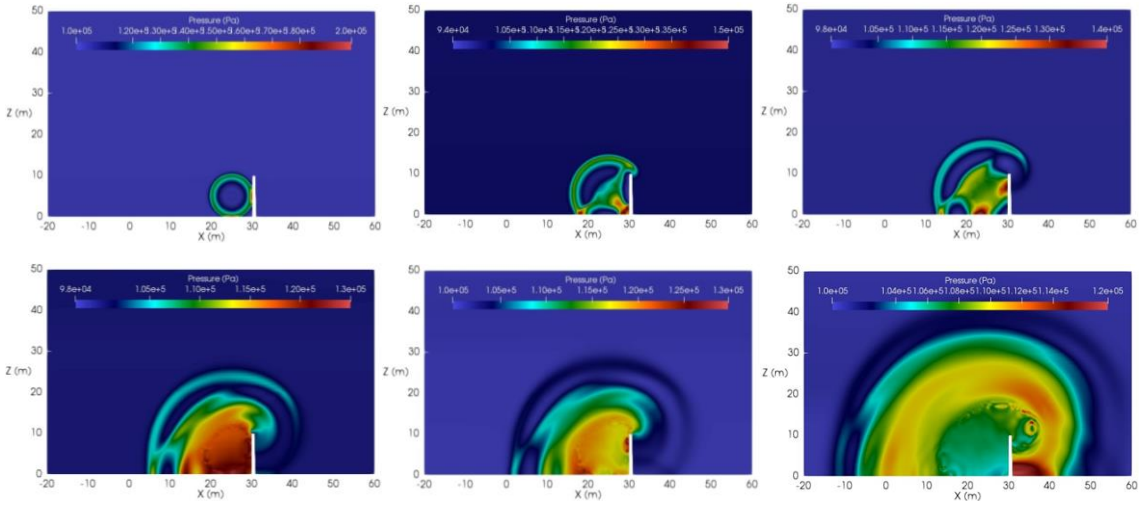

Figure 7. Predicted contours of pressure in the middle plane for the case of IR10 at a time sequence of 10 ms, 20 ms, 30 ms, 50 ms, 60 ms, 100 ms after the ignition.

Figure 7 shows the pressure evolution in the middle after the ignition for the case with a 10 m barrier wall. The ignition process produces a strong blast wave emitting from the ignition point. It was found

that the strength of this blast wave is affected by the size and temperature increasing rate of the ignition source. This initial blast wave is reflected from both the ground and barrier wall and propagates outwards, quickly dying out at 60 ms after the ignition. Meanwhile another blast wave caused by the fast deflagration is initiated and catching up with the first blast wave. The second blast wave passes the barrier wall and is reflected from the ground behind the barrier wall, creating a local high-pressure region.

Figure 8 shows the temperature evolution in the middle plane after the ignition for the case with a 10 m barrier wall. The predicted spherical ignition kernel grows quickly due to the deflagration. The initial flame propagation speed is roughly 55 m/s, and the flame propagates both downstream and upstream with a gradually reduced flame speed. The flame overcomes the wind speed, propagating towards the release point. In addition, the flame goes around the barrier wall, propagating further downstream.

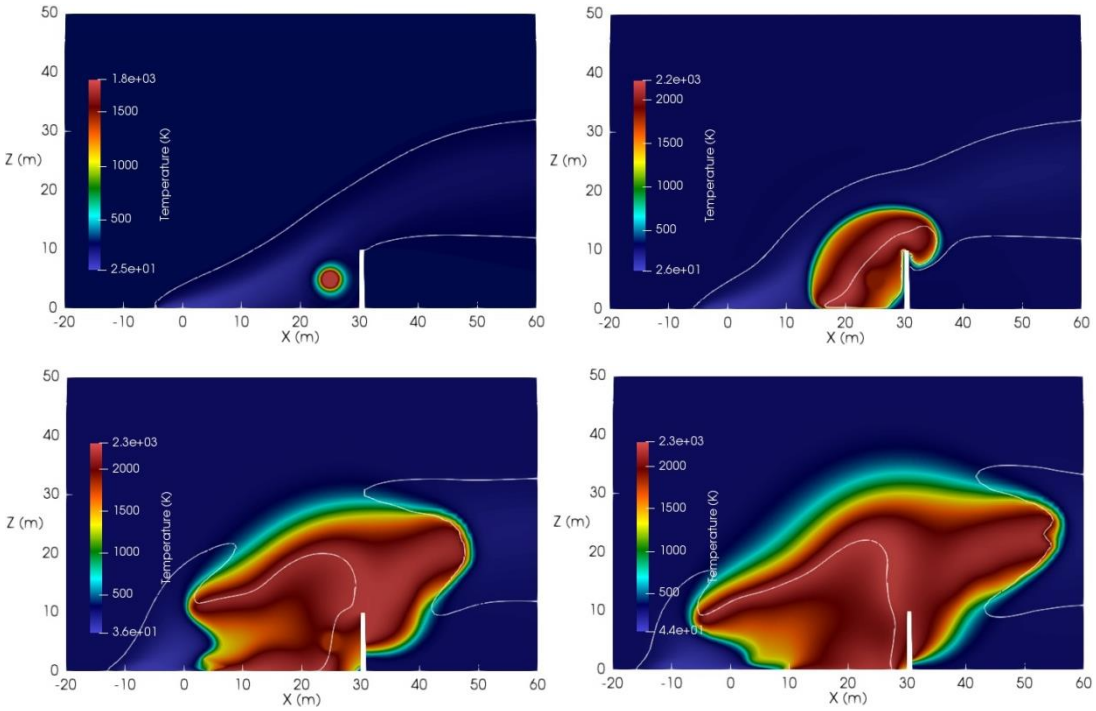

Figure 8. Predicted contours of temperature in the middle plane for the case of IR10 at a time sequence of 10 ms, 100 ms, 500 ms, 1000 ms after the ignition.

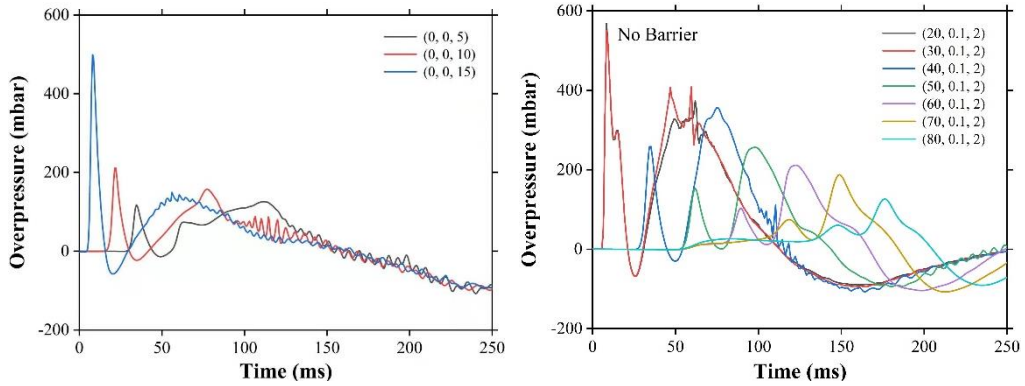

Figure 9. Predicted over-pressures at different monitoring points for the cases of IR9 (left) and IR10 without barrier walls.

Figure 9 shows the predicted over-pressures at different monitoring points for the cases of IR9 and IR10 without barrier walls. The ignition source is located at (0, 0, 20) for the case of IR9. The first peak for

all the monitoring points of the case of IR9 is caused by the ignition process, attenuates quickly away from the ignition location. The second peaks of the case of IR9 are caused by the fast deflagration, which also gradually decreases away from the ignition point. The negative over-pressure is caused by the thermal expansion. The overpressure caused by the deflagration can be as high as 400 mbar for the case of IR10, much higher than that of the case of IR9.

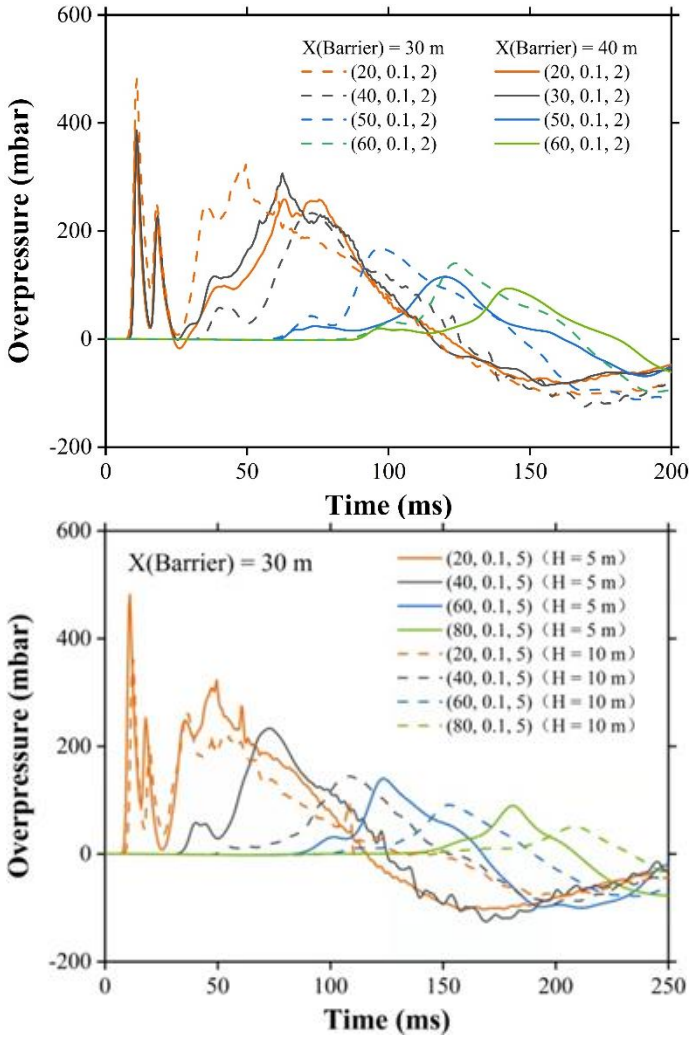

Figure 10. Predicted over-pressures at different monitoring points for the case of IR10 with barrier walls of different heights and locations (Top: comparison of different locations of a 5 m height barrier wall, Bottom: comparison of different heights of a barrier wall located at x = 30 m).

Figure 10 show the predicted over-pressures at different monitoring points for the case of IR10 with barrier walls of different heights and locations. The barrier wall can significantly reduce the downstream over-pressure. A barrier wall close to the ignition location will increase the both upstream and downstream over-pressures due to the reflection of the blast wave. A barrier wall away from the ignition location will delay the arrival of the blast wave caused by the deflagration. A barrier of a large height wall can reduce the downstream over-pressure and delay the arrival of the blast wave caused by the deflagration. It is worth noting that a significant negative over-pressure of approximately 100 mbar also exists due to the thermal expansion.

CONCLUSIONS

The in-house HyFOAM code has been further modified to simulate cryogenic hydrogen releases related to LH_2 storage and refueling. The code is now capable of simulating hydrogen releases at cryogenic conditions and the subsequent atmospheric dispersion and ignition. Predictions have been conducted for the fields of temperature and hydrogen concentration of both horizontal and vertical jets, considering the effect of release orientation, wind speed, ambient temperature, and release content, etc. The effect of a barrier wall on the vapour cloud explosions following catastrophic releases was also studied. The major findings are summarized as follows.

1. A horizontal jet release is initially momentum-dominant and gradually loses its momentum due to the mixing with ambient air and then shows a buoyant effect. The buoyancy effect is significantly restrained by a concurrent wind condition. A strong wind condition also greatly enhances the mixing, reducing the size of the dispersed cloud.
2. The release momentum of a vertical jet release is in alignment with the buoyancy force, the jet flow slowly decays upwards. A strong cross wind greatly enhances the mixing, resulting in a quick decay of the release momentum. The predicted cloud turns to be horizontal and quickly disperses into the ambient air.
3. A horizontal jet fire quickly transitions to be buoyancy-dominant under no wind condition. Under a wind condition the buoyant effect is significantly reduced and a tilted long jet fire is formed.
4. Ignition of a dispersed cloud resulting from an instantaneous release produces a fast deflagration and strong blast wave. The blast wave can pass a barrier wall and propagate downstream.
5. The initial flame can be as high as 55 m/s. The flame overcomes the wind speed, propagating towards the release point. In addition, the flame goes around the barrier wall, propagating further downstream.
6. The barrier wall can significantly reduce the downstream over-pressure. A barrier wall close to the ignition location will increase the both upstream and downstream over-pressures. A barrier wall away from the ignition location will delay the arrival of the blast wave caused by the deflagration. A barrier of a large height wall can reduce the downstream over-pressure and delay the arrival of the blast wave caused by the deflagration.

RECOMMENDATIONS

According to the findings of this study, the following recommendations are made for safety zones and mitigation measures.

1. Upward venting of LH_2 is recommended to increase the safety zones instead of horizontal venting.
2. To void accumulation of high concentration of flammable cloud, sufficient ventilation is required to quickly dilute the flammable cloud.
3. To reduce explosive hazards, a barrier wall of sufficient height is recommended but this needs to be considered in combination with the effect on explosion overpressure.
4. The barrier wall should be kept a sufficient distance away from potential ignition sources.
5. A sufficient safety distance to protect personnel is required due to the existence of extremely low temperature zone 10 m beyond the potential release points based on the release scenarios and environmental conditions considered in this study.

It is strongly recommended that for specific development of hydrogen refueling infrastructure at airports,

similar analysis should be conducted with the relevant release scenarios, environmental conditions, and geometric layouts.

ACKNOWLEDGEMENT

The work reported here is funded by the UK Transport Research Innovation Grants ZERO EMISSION FLIGHT (TREG-ZEF) on "Safety zones and mitigation measures for hydrogen refuelling infrastructure at airports" (2021 - 2022). The numerical simulations were conducted using EPSRC supercomputer ARCHER 2 through "Addressing Challenges Through Effective Utilisation of High Performance Computing - a case for the UK Consortium on Turbulent Reacting Flows (UKCTRF EP/R029369/1).

REFERENCES

1. R.D. Witcofski, and J.E. Chirivella, Experimental and analytical analyses of the mechanisms governing the dispersion of flammable clouds formed by liquid hydrogen spills, Int. J. Hydrogen Energ. 9, 1984, 425-435.
2. Jordan, T., Bernard, L., Cirrone, D., Coldrick, S., Friedrich, A., Jallais, S., Kuznetsov, M., Proust, C., Venetsanos, A. and Wen, J.X., Results of the pre-normative research project Preslhy for the safe use of liquid hydrogen, Ebook - ICHS 2021 – September 2021.
3. K Lyons, S Coldrick, G Atkinson, Ignited releases, PRESLHY dissemination conference, 5-6 May 2021, online event.
4. ZX Ren, IX Wen, Numerical characterization of under-expanded cryogenic hydrogen gas jets. AIP Advances, 2020, 10 (9).
5. SG Giannissi, A G Venetsanos, ES Hecht, Numerical predictions of cryogenic hydrogen vertical jets, *Int. J. Hydrog. Energy, 2021,* 46:12566-12576.
6. Z.X. Ren, S. Giannissi, A.G. Venetsanos, A. Friedrich, M. Kuznetsov, T. Jordan, J.X. Wen, The evolution and structure of ignited high-pressure cryogenic hydrogen jets, Int. J of Hydrogen Energy, 2022, 47(67): 29184-29194.
7. DMC Cirrone, D Makarov, V Molkov, Thermal radiation from cryogenic hydrogen jet fires, *Int. J. Hydrog. Energy, 2019, 44:8874-8885.*
8. BP Xu, S Jallais, D Houssin, E Vyazmina, L Bernard, JX Wen, Numerical simulations of atmospheric dispersion of large-scale liquid hydrogen releases Ebook - ICHS 2021 – September 2021.
9. K Verfondern, B Dienhart, Experimental and theoretical investigation of LH_2 pool spreading &vaporization. *Int J Hydrogen Energy, 1997, 22(7):649-660.*
10. AV Shelke, JX Wen, The burning characteristics and flame evolution of hydrocarbon and hydrogen flash fires. Proc. of the Combustion Institute. 38(3), 2020.
11. CMR Vendra, P Sathiah, JX Wen, Effects of congestion and confining walls on turbulent deflagrations in a hydrogen storage facility-part 2: numerical study. Int. J of Hydrogen Energy, 2018, 43 (32).